

## Effect of higher frequency on the classification of steady-state visual evoked potentials

This content has been downloaded from IOPscience. Please scroll down to see the full text.

2016 J. Neural Eng. 13 016014

(<http://iopscience.iop.org/1741-2552/13/1/016014>)

View [the table of contents for this issue](#), or go to the [journal homepage](#) for more

Download details:

IP Address: 163.152.73.54

This content was downloaded on 23/12/2015 at 11:50

Please note that [terms and conditions apply](#).

# Effect of higher frequency on the classification of steady-state visual evoked potentials

Dong-Ok Won<sup>1</sup>, Han-Jeong Hwang<sup>2</sup>, Sven Dähne<sup>2</sup>,  
Klaus-Robert Müller<sup>1,2</sup> and Seong-Whan Lee<sup>1,3</sup>

<sup>1</sup>Department of Brain and Cognitive Engineering, Korea University, Anam-dong, Seongbuk-ku, Seoul, Korea

<sup>2</sup>Machine Learning Group, Technical University of Berlin, Berlin, Germany

E-mail: [wondongok@korea.ac.kr](mailto:wondongok@korea.ac.kr), [han-jeong.hwang@tu-berlin.de](mailto:han-jeong.hwang@tu-berlin.de), [sven.daehne@tu-berlin.de](mailto:sven.daehne@tu-berlin.de), [klaus-robert.mueller@tu-berlin.de](mailto:klaus-robert.mueller@tu-berlin.de) and [sw.lee@korea.ac.kr](mailto:sw.lee@korea.ac.kr)

Received 30 May 2015, revised 12 November 2015

Accepted for publication 16 November 2015

Published 23 December 2015



CrossMark

## Abstract

*Objective.* Most existing brain–computer interface (BCI) designs based on steady-state visual evoked potentials (SSVEPs) primarily use low frequency visual stimuli (e.g., <20 Hz) to elicit relatively high SSVEP amplitudes. While low frequency stimuli could evoke photosensitivity-based epileptic seizures, high frequency stimuli generally show less visual fatigue and no stimulus-related seizures. The fundamental objective of this study was to investigate the effect of stimulation frequency and duty-cycle on the usability of an SSVEP-based BCI system.

*Approach.* We developed an SSVEP-based BCI speller using multiple LEDs flickering with low frequencies (6–14.9 Hz) with a duty-cycle of 50%, or higher frequencies (26–34.7 Hz) with duty-cycles of 50%, 60%, and 70%. The four different experimental conditions were tested with 26 subjects in order to investigate the impact of stimulation frequency and duty-cycle on performance and visual fatigue, and evaluated with a questionnaire survey. Resting state alpha powers were utilized to interpret our results from the neurophysiological point of view. *Main results.* The stimulation method employing higher frequencies not only showed less visual fatigue, but it also showed higher and more stable classification performance compared to that employing relatively lower frequencies. Different duty-cycles in the higher frequency stimulation conditions did not significantly affect visual fatigue, but a duty-cycle of 50% was a better choice with respect to performance. The performance of the higher frequency stimulation method was also less susceptible to resting state alpha powers, while that of the lower frequency stimulation method was negatively correlated with alpha powers. *Significance.* These results suggest that the use of higher frequency visual stimuli is more beneficial for performance improvement and stability as time passes when developing practical SSVEP-based BCI applications.

Keywords: brain–computer interface, electroencephalogram, steady state visual evoked potentials, visual fatigue

(Some figures may appear in colour only in the online journal)

<sup>3</sup> Author to whom any correspondence should be addressed.

## 1. Introduction

A brain–computer interface (BCI) is an important communication tool for individuals with neurological disorders or motor disabilities, such as amyotrophic lateral sclerosis or spinal cord injury. Since the electroencephalograph (EEG) has a high temporal resolution and its recording system is cost-effective compared to other neuroimaging modalities, BCI systems primarily use EEG signals non-invasively recorded from human scalps. One of the most widely studied applications of EEG-based BCI is the BCI speller [1–4], which allows those with locked-in states (e.g., due to paralysis) to express their thoughts by attending to target characters [5–8].

Recently, some BCI studies have shown that BCI spelling systems can be implemented using steady-state visual evoked potentials (SSVEPs) [9–13]. Most studies have introduced promising approaches to increase the spelling speed of SSVEP-based BCI spellers by employing a real-time neuro-feedback mechanism to increase attention on visual stimuli [14] and hybridizing the P300 paradigm with the SSVEP paradigm [15]. However, this remains a challenging issue in the field of BCI research [16–19]. Using SSVEP provides a very reliable communication paradigm for the implementation of a non-invasive BCI system [18–20].

However, an SSVEP-based system can cause visual fatigue due to flickering visual stimuli presented to evoke SSVEPs. In particular, low frequency visual stimuli are more apt to cause excessive visual fatigue [21]. While visual stimuli flickering with a frequency between 4 and 90 Hz can elicit SSVEPs, lower frequency visual stimuli tend to induce higher SSVEP responses than high frequency stimuli [22]. Therefore, many SSVEP-based BCI applications have adopted relatively low frequency bands for visual stimulation (e.g., <20 Hz) [10]. However, although high frequency stimuli generally induce a lower amplitude SSVEP response, the signal-to-noise ratio (SNR) of the SSVEP responses is not significantly inferior [18, 23, 24]. Moreover, it has been confirmed that higher frequency SSVEP-based BCIs are less susceptible to visual fatigue [21]. Recently, several studies used higher stimulation frequencies in SSVEP-based BCI applications [21, 25]. For example, Diez *et al* [21] utilized a BCI system with cursor control that employed four high frequencies (36, 37, 38, and 39 Hz). Lin *et al* [26] developed an SSVEP-based BCI system using nine frequencies (27, 29, 31, ..., 43 Hz). In addition, several recent BCI studies found visual comfort to be associated with the duty-cycle of the flickering stimuli in SSVEP-based BCI systems [23, 24].

Several studies employed high frequency stimuli for SSVEP-based BCIs [21, 25, 27, 28] in order to induce less visual fatigue and avoid the risk of inducing photoepileptic seizures and interfering with the alpha rhythm. Other relevant studies allowed variable frequency stimuli ranges, such as low to medium (6–24 Hz, 6–25 Hz, 14–29 Hz, and 7–35 Hz) [29–32], low to high (8.8–35 Hz, 8–48 Hz, 10–50 Hz) [33–35], and medium to high (27–43 Hz) [26]. There are also SSVEP-based BCI studies that compared the performance or SNRs of low (e.g., <20 Hz) and high (e.g.,

>20 Hz) frequency stimulation methods [28, 36]. See also the reviews in [37, 38] for an overview of SSVEP properties. However, to the best of our knowledge, there have been no studies to date which directly compare the performance trends of low and high frequency stimuli in terms of time, which is an important factor to be investigated for long-term use of a BCI system.

In our study, we implemented an SSVEP-based speller that utilized either low frequency stimuli (6–14.9 Hz) with a duty-cycle of 50% or higher frequency stimuli (26–34.7 Hz) with different duty-cycles of 50%, 60%, and 70%. We also applied different kinds of duty-cycle (50%, 60%, and 70%) to our design, as this could potentially reduce visual fatigue. In addition, we used a questionnaire survey, which was based on a previous study [24], in order to evaluate the psychological feelings of visual comfort in response to different frequencies and duty-cycles. Finally, we evaluated the changes of performance in this SSVEP-based BCI system across time. This is an important aspect, because real-life application of BCI-based systems requires their performance to be robust.

## 2. Methods

### 2.1. Experiment Setup

**2.1.1. Participants.** The experiment included 26 healthy participants (22 male and four female; aged  $27.2 \pm 2.5$ ). All the participants had no history of visual disorders and had either normal or corrected-to-normal vision. All the experiments were conducted according to the principles described in the Declaration of Helsinki. This study was reviewed and approved by the Institutional Review Board at Korea University (1040548-KU-IRB-15-8-A-1). Written informed consent was obtained from all participants prior to the experiment.

**2.1.2. Stimulator design.** A stimulator layout was designed in the QWERTY-style speller (figure 1). Previous research has shown that familiar layouts (e.g., QWERTY) are preferable to unfamiliar layouts [13]. The layout consisted of 30 LED lights which represented the 26 English alphabet letters and four symbols (‘.’, ‘<’, ‘-’, and ‘/’) rather than the words ‘dot’, ‘backspace’, ‘space’, and ‘enter’. The compact QWERTY board was 280 x 85 mm, each LED light source was 5 mm in diameter, and the gap between the neighboring stimuli was 30 mm. Individual characters were printed on a diaphanous paper to label each target character, and the diaphanous paper was placed in front of the LED controller board. Thirty LEDs were then attached behind the diaphanous paper to diffuse the emitted light.

A frequency array was specifically designed for the LED lights (figure 2), such that the minimum difference between neighboring LEDs was 1.2 Hz. For example, in the case of the letter ‘G’ and its flickering frequency, the neighboring LEDs (‘T’, ‘Y’, ‘F’, ‘H’, ‘V’, and ‘B’) had frequency differences of 1.7, 6.5, 5.3, 5.0, 1.2, and 3.8 Hz, respectively. This LED array has adjustable flickering frequencies with precise

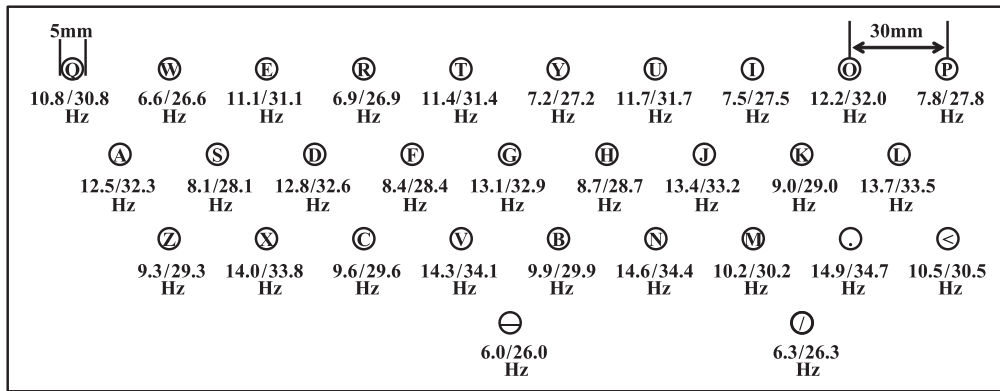


**Figure 1.** Speller layout design and frequency arrangements. Left: low frequencies (6–14.9 Hz). Right: higher frequencies (26–34.7 Hz).

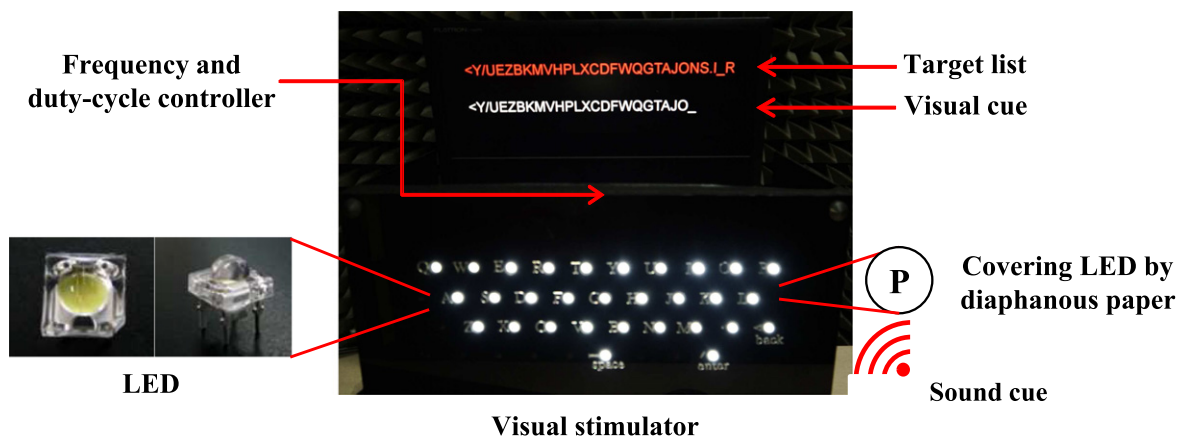


**Figure 2.** The experimental setup. See the supplementary movies (available from [stacks.iop.org/JNE/xx/xxx/mmedia](http://stacks.iop.org/JNE/xx/xxx/mmedia)) to view the scenes of the experiment. The first line on the screen represents the target characters the user should spell during the experiment, and the second line shows the characters the user attempted to spell and the current target (‘N’ in the figure) the user is trying to spell, respectively.

frequency ranges to avoid the visual fatigue caused by 4–15 Hz stimuli and the photosensitivity-based epileptic seizures evoked by 15–25 Hz stimuli [39].

**2.1.3. Visual stimuli setup and validation.** We used square multi-chip LEDs with high flux (part number: DG-82A83C-001-5/S-3; emitting color: white; lens color: water; luminous intensity of 6000 mcd; peak wavelength: 0.26/0.28 nm; operating current: 20 mA). The LED controller was built using an NI CompactDAQ USB data acquisition system (model: cDAQ-9174, National Instruments) and digital output module (model: NI 9476, National Instruments). The stimuli were placed 65–75 cm in front of the participants in the study. The maximum variation was  $\pm 0.1$  Hz for the higher frequencies (26–34.7 Hz), and  $\pm 0.01$  Hz for low frequencies (6–14.9 Hz). The increased maximum variation for the higher frequency stimulation was caused by an inherent limitation of the hardware system, where a shorter time is given for presenting a higher frequency stimulus (100 ms for 10 Hz versus 40 ms for 25 Hz for one cycle of turning an LED on

and off). Note that the maximum variation of 0.1 Hz for the higher frequency stimulation did not significantly affect experimental results because a frequency span of 0.3 Hz was used in this study for the higher frequency stimulation.

In this study, we tested three different duty-cycles (50%, 60%, and 70%) in the higher frequency stimulation conditions. A higher duty-cycle stimulus at the same stimulation frequency uses a higher light energy in the same stimulation conditions because an LED is turned on for a longer time. This generally induces stronger SSVEP responses because the eyes are exposed to a visual stimulus for longer [40], which hampers a fair performance comparison for different stimulation conditions using duty-cycles of 50%, 60%, and 70%. Thus, we used different resistances that guaranteed the use of an almost identical amount of light power for the three duty-cycle conditions (e.g., 50%: 120 ohms ( $\Omega$ ), 0.0349 wattage (W); 60%: 144  $\Omega$ , 0.0344 W; 70%: 168  $\Omega$ , 0.0344 W). A higher resistance was used for a higher duty-cycle stimulus to reduce the brightness of the LED stimulus appropriately, thereby making the different duty-cycle stimuli use an almost identical amount of light energy.

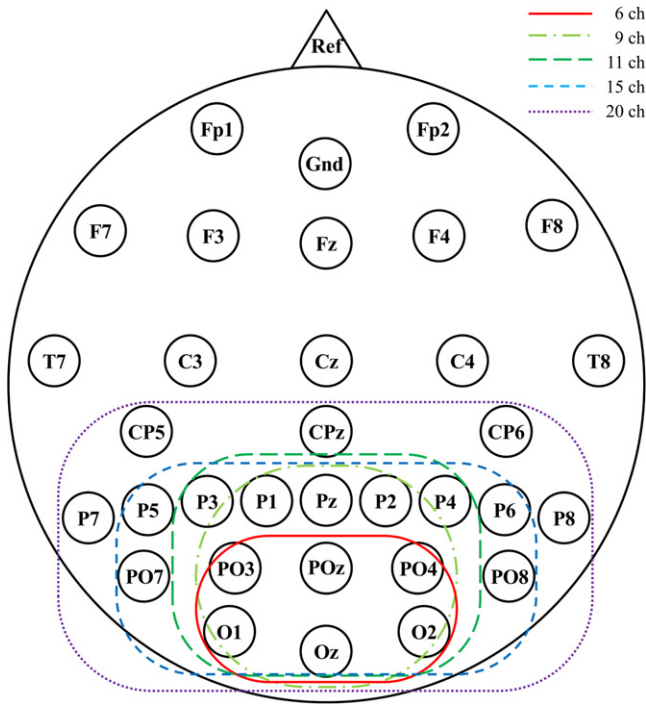


Figure 3. Channel configurations.

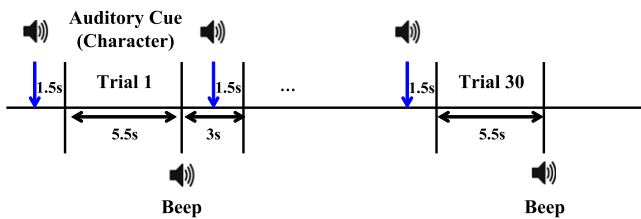


Figure 4. The timeline of the experimental paradigm.

2.2. Data acquisition

EEG data were recorded from 32 electrodes attached according to the international 10–20 system using BRAINAMP (Brain Products, Germany) (figure 3). Because strong SSVEPs are mainly observed on the back of the head, the recording electrodes were placed most densely over the occipital lobe. Prior to the experiment, EEG signals were recorded for 60 s to assess the brain’s resting state activation. There are four different experimental conditions: low frequency stimuli with duty-cycle 50% (LFS 50), higher frequency stimuli with duty-cycle 50% (HFS 50), higher frequency stimuli with duty-cycle 60% (HFS 60), and higher frequency stimuli with duty-cycle 70% (HFS 70). Conditions with a duty-cycle of less than 50% were not employed, as they are associated with high visual fatigue [24]. All the subjects performed four experimental sessions, denoted A, B, C, and D. Each session included four experimental runs. Session A comprised LFS50, HFS50, LFS50, and HFS50 runs. Session B consisted of HFS50, LFS50, HFS50, and LFS50 runs. Session C comprised HFS60, HFS70, HFS60,

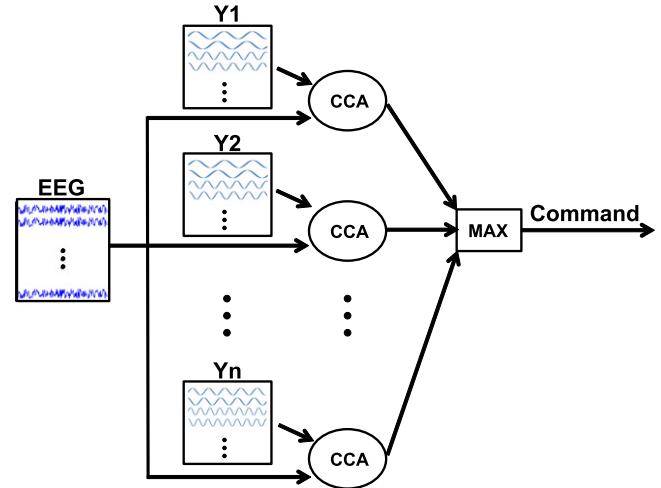


Figure 5. An illustration of CCA used in EEG signal analysis.

and HFS70 runs, and session D used HFS70, HFS60, HFS70, and HFS60 runs. The order of sessions was either A, C, B, and D or D, B, C, and A to alternatively test the four experimental conditions. The counterbalanced experiment could prevent potentially biased results for the two independent factors, stimulation frequency, and duty-cycle. Furthermore, the first session order (A, C, B, and D) was used for almost half of the subjects (12 of 26 subjects), and the second one (D, B, C, and A) was used for the others for more counterbalancing of the experiment. In each experimental run, participants were asked to spell all 30 characters once with a random order, for which verbal instruction was used. The time used for spelling one character was 5.5 s, and a break of 3 s was given between characters (figure 4). All data analyses were conducted off-line after the experiment.

2.3. EEG Data analysis

In the past, a simple target detection algorithm, called power spectral density analysis (PSDA), was used in which a stimulus modulated with the frequency showing the strongest amplitude is selected as a target stimulus. However, PSDA is sensitive to noise due to the use of single or bipolar channels [26]. Many methodologies have been introduced to overcome this limitation of PSDA. One of these is the canonical correlation analysis (CCA)-based SSVEP recognition introduced by Lin *et al* [26], which has been shown to yield better performance than PSDA. In addition, CCA has an advantage of subject independence [41].

Figure 5 illustrates the concept of the CCA algorithm for frequency recognition in the SSVEP-based BCI. CCA, a multi-variable statistical method, maximizes the correlation between two sets of variables by means of linear combinations [42–44]. In the case of SSVEP BCI, the sets of variables are: the recorded EEG data of an individual trial, denoted by  $X$ , and a set of reference signals for each stimulus, denoted by

**Table 1.** Accuracy of channel-wise and stimulus-wise average performance results.

Stimulus	6 ch	9 ch	11 ch	15 ch	20 ch	Average
LFS 50	60.1	62.0	62.0	66.5	65.0	63.1
HFS 50	59.2	65.0	66.3	68.9	68.7	65.6
HFS 60	51.1	58.8	58.2	60.0	59.8	57.6
HFS 70	36.9	41.1	40.9	44.0	42.8	41.1
Average	51.8	56.7	56.9	59.9	59.1	

$Y_i$ . The reference signal  $Y_i$  is defined as

$$Y_i(t) = \begin{pmatrix} \sin(2\pi f_i t) \\ \cos(2\pi f_i t) \\ \sin(2\pi 2f_i t) \\ \cos(2\pi 2f_i t) \\ \dots \\ \sin(2\pi Hf_i t) \\ \cos(2\pi Hf_i t) \end{pmatrix}$$

,where  $f_i$  is the flickering frequency of the  $i$ th stimulus and  $H$  is an integer denoting the number of harmonics to be included. CCA is applied to maximize the correlation between the EEG data of a given trial,  $X$ , and the reference signals of the  $i$ th stimulus,  $Y_i$ , separately for each stimulus. The obtained correlation is denoted by  $\rho_i$ . The user's command  $C$  is then defined as the stimulus index for which the correlation between the EEG data and the reference signals was highest.

To find the best electrode configuration for the main analysis, we considered five different electrode configurations focused on the occipital areas, as illustrated in figure 3. These channel configurations were selected based on previous SSVEP studies [17, 26, 41]. The six-channel configuration included PO3, POz, PO4, O1, Oz, and O2, with which nine-, 11-, and 15-channel configurations sequentially included the following channels according to the number of electrodes, P1, Pz, P2, P3, P4, P5, P6, PO7, and PO8, respectively. For the main analysis, the 15-channel configuration was used because this configuration showed the highest mean classification performance over different stimulation conditions (see table 1 for detailed results).

The classification results were correlated with the average magnitude of the alpha rhythm, measured in the resting state prior to the BCI task [45, 46]. To generate a more stable resting state measure, we used the last 45 s of the 1 min resting state recording. For all the subjects, the alpha range was defined to be 7.5–12.5 Hz and then divided into *alphaLow* (7.5–9 Hz) and *alphaHigh* (9–12.5 Hz) [45]. The band power of alphaLow and alphaHigh over occipital electrodes (PO3, POz, PO4, O1, Oz, and O2) was normalized by dividing it with the respective band power averaged over all the scalp electrodes.

## 2.4. Questionnaire survey

A questionnaire survey was conducted to evaluate the subjective comfortableness of the visual stimuli with respect to the frequency band and duty-cycle. The questionnaire used a five-level satisfaction rating score of '1—unacceptable', '2—uncomfortable', '3—acceptable', '4—comfortable', and '5—delightful'. The participants filled in the questionnaire after each run without having information about the run sequences during the experiments [24]. Because all the subjects performed 16 experimental runs (four stimulation conditions x four times) and rated visual fatigue level after each run, a total of 104 evaluation results (26 subjects x four stimulation conditions) were obtained for each category of stimulation conditions (LFS 50, HFS 50, HFS 60, and HFS 70).

## 3. Results

The performance attained with different electrode configurations (six, nine, 11, 15, and 20 channels) was compared. Because the performance was the most dominant when using 15 channels, only this channel configuration was used for further analysis (table 1). The average detection accuracies for LFS 50, HFS 50, HFS 60, and HFS 70 were 66.5%, 68.9%, 60.0%, and 44.0%, respectively when using the 15-channel configuration (chance level: 3.33 %). The mean accuracy was comparable between high and low frequency SSVEP systems across the participants and channel selections (table 1). A one-way repeated measures ANOVA with factor (four stimulus conditions) a significant effect ( $F = 4.91$ ,  $p < 0.01$ ) was conducted. There was a significant difference between LFS 50 and HFS 70, and between HFS 50 and HFS 70, but there were no significant differences between HFS 60 and the other conditions (LFS 50, HFS 50, and HFS 70). The average accuracy decreased with higher frequency (26–34.7 Hz) with duty-cycle 50%, 60%, and 70% stimuli conditions (average accuracy: HFS 50 > HFS 60 > HFS 70). Figure 6 shows the accuracy of all the participants using 15 channels for 6–14.9 Hz with a duty-cycle of 50% and 26–34.7 Hz with duty-cycles of 50%, 60%, and 70%.

Figure 7 depicts the participant averages for the 30 target trials in consecutive order and experimental sequence, in order to show the changes in accuracy as a function of time. Figures 7(a) and (b) show the changes in the ratio of the target and non-target  $\rho$ -values and the classification accuracy as a function of the trial sequence for the four stimulation conditions. The two measures show similar trends within the stimulus conditions.

The slope of a linear trend was estimated for the changes in SNR, accuracy, and target band power. The estimated target band power slopes were  $-0.2671$  for LFS 50,  $0.2532$  for HFS 50,  $0.2913$  for HFS 60, and  $-0.0928$  for HFS 70. Further, the estimated accuracy slopes were as follows:  $-0.4710$  for LFS 50,  $0.0466$  for HFS 50,  $0.0990$  for HFS 60, and  $-0.0009$  for HFS 70. These results suggest that there is a trend of decreasing SNR, accuracy, and target band power for the LFS 50 conditions along time. By contrast, the higher

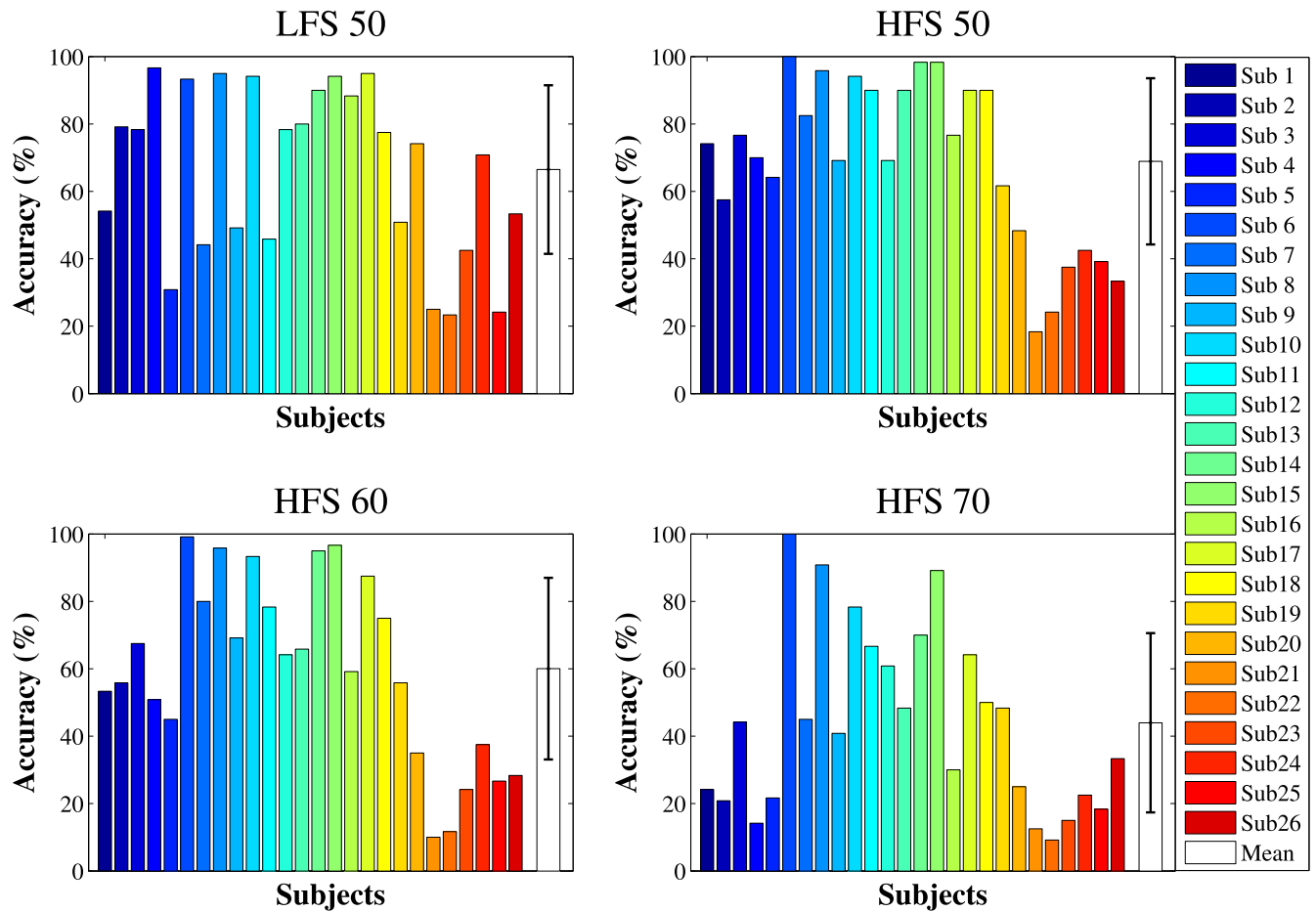


Figure 6. The accuracy of classification for different flickers (LFS 50, HFS 50, HFS 60, and HFS 70).

frequency conditions yielded relatively stable SNR, performance, and band power. Higher frequency stimuli conditions with duty-cycles of 50% and 60% did not exhibit a severe drop in performance as the experiments proceeded.

Figure 8 displays the averaged distribution of the SSVEP amplitudes elicited by LFS 50 and HFS 50; the red colored lines indicate a stronger SSVEP, which exhibit different patterns, particularly when analyzing merged trial bins (e.g., 1 to 10 trials, 11 to 20 trials, and 21 to 30 trials). In particular, the topography of the low frequency stimuli indicated less spectral power in the occipital region.

The occipital alpha rhythm was negatively correlated with the classification accuracy in low stimulus frequency conditions, while there was no significant correlation between the alpha power and performance in the high stimulus frequency conditions. The results of this analysis are shown in table 2, where  $r$  denotes the correlation coefficient and  $p$  denotes the significance level of the correlation coefficient.

Figure 9(a) shows the alphaLow power and the classification performance across subjects. In this figure, the subjects have been ordered according to resting state alphaLow in ascending order. It can be seen that the resting state alphaLow only predicts the BCI performance for low stimulus frequency conditions, and not for higher stimulus frequencies.

The results of the questionnaire survey regarding visual fatigue are shown in table 3. No participants reported ‘delightful’ with low frequency conditions, while no participants reported an ‘unacceptable’ rating for the higher frequency conditions during the experiments. Visual fatigue was quantified using the satisfaction score, such that a smaller number represented greater fatigue, as ‘unacceptable’ was scored as a 1 and ‘delightful’ as a 5. The majority considered participation in the low frequency experiment to be ‘uncomfortable’, while participation in the experiment with the higher frequency with duty-cycles of 50%, 60%, and 70% stimuli was considered to be between ‘acceptable’ and ‘comfortable’. There were no or minimal differences in visual comfort for higher frequency with duty-cycles of 50%, 60%, and 70% stimuli.

Visual fatigue satisfaction scores for the four conditions (LFS 50, HFS 50, HFS 60, and HFS 70) were obtained from the visual fatigue questionnaire survey (figure 10). As depicted in figure 10, HFS 70 achieved slightly higher satisfaction rates than the other higher frequency conditions. A one-way repeated measures ANOVA with factor (four stimulus conditions) a significant effect ( $F = 27.05$ ,  $p < 0.01$ ) was conducted. There was a significant difference between the low frequency (LFS 50) and higher frequency

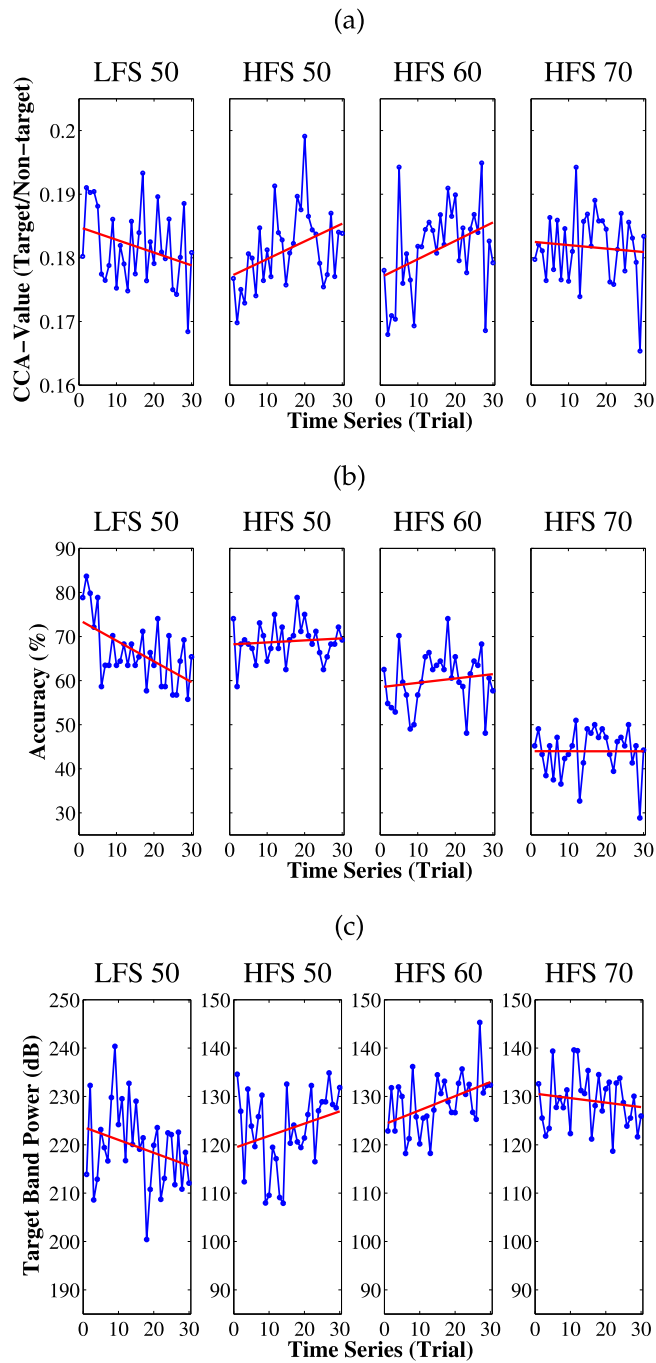


**Figure 7.** Comparison of (a) SNR, (b) accuracy, and (c) target band power trend as a function of trial sequence.

stimuli (HFS 50, HFS 60, and HFS 70), but no significant differences between the HFS 50, HFS 60, and HFS 70 conditions (visual comfort: LFS 50 < HFS 50 = HFS 60 = HFS 70). According to the visual fatigue questionnaire survey, the average satisfaction scale for all participants regarding HFS 50, HFS 60, and HFS 70 conditions was 3.5, which translates to a rating between ‘acceptable’ and ‘comfortable’. Moreover, the average satisfaction scale in low frequency stimuli was 2.4, which is a rating closer to ‘uncomfortable’. Therefore, there was an effective reduction of visual fatigue with higher frequency stimuli.

#### 4. Discussion

In this study, we implemented an SSVEP-based BCI speller with 30 characters to investigate the impact of stimulation frequencies on system performance and visual fatigue. We demonstrated that the SSVEP system design employing the high frequency band yielded higher accuracy and lower discomfort levels, compared to low frequency stimulation. Our study is the first to assess performance and comfort differences between high and low frequency stimuli in SSVEP BCIs in the same group of subjects. In other studies, low frequency was noted as having high amplitude and high SNR, more so than high frequency [18, 21]. Therefore, low frequency stimuli have been used for most SSVEP BCI studies, despite the possibility of extreme visual fatigue. To date, no studies have investigated the fluctuations of SSVEP performance over time, which is critical for the development of stable and robust BCIs in real-world applications. We analyzed the trend of SSVEP performance as a function of time (figure 7), and obtained a similar averaged accuracy in LFS 50 (6–14.9 Hz), HFS 50, HFS 60, and HFS 70 (26–34.7 Hz) conditions (figure 6). However, we detected a difference in performance among different frequencies, by comparing the average performance between the first and the last trials (figure 7). Low frequency stimuli led to a decrease in performance, but a higher frequency led to stable performance. From this, we can conclude that there are performance losses as time passes when low frequency SSVEP is adopted. Therefore, while the high SNR of low frequency SSVEP is valid, it does not assure high performance for long-time use in real-life BCI applications. It may be advantageous to use higher frequency SSVEP because it showed more stable performance, even during short time frames (e.g., 5 min), unlike low frequency SSVEP.

Previously, BCIs using high frequency conditions were considered only to be visually comfortable [21, 25, 27, 28, 36]. However, we demonstrated that a higher frequency stimulus not only reduced the visual fatigue problem, but also improved performance as time passed, demonstrating that higher frequency conditions are more suitable than low frequency for BCI applications. Note that the majority of the relevant studies still use low frequency bands for stimulation due to the higher SNRs, although there are several disadvantages in terms of ergonomics. We recommend using higher frequencies when applying SSVEP-based BCIs for real-world use because of better performance and stability as time passes, and greater visual comfort.

Several recent BCI studies which analyzed visual fatigue in SSVEP-based BCI systems found that visual comfort was susceptible to stimulation frequencies [10, 18] and duty-cycles [23, 24]. Lee *et al* used a 13.16 Hz visual stimulus with different duty-cycle flickers, such as 10% to 90% duty-cycles, and found that higher duty-cycle flickers achieved greater visual comfort [24]. To our knowledge, there have been no studies comparing duty-cycle flickers of higher frequency (26–34.7 Hz) stimuli in SSVEP-based BCIs. Therefore, we investigated this system’s performance and visual comfort using various duty-cycle flickers (50%, 60%, and 70%) of

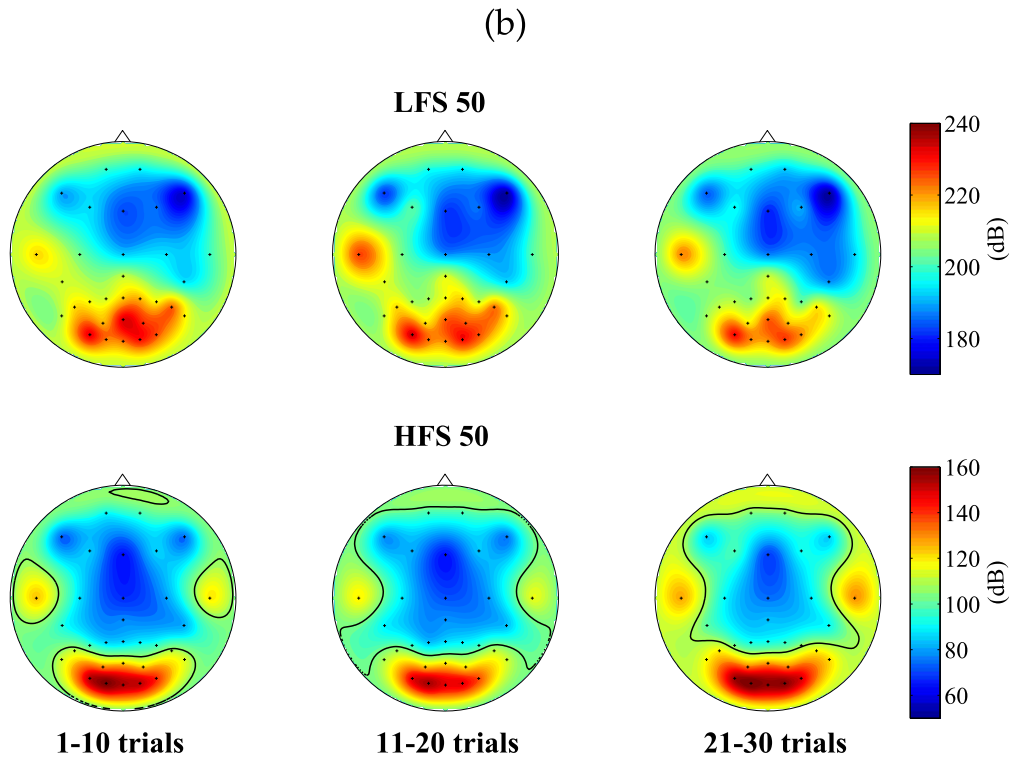


**Figure 8.** Grand-average topographical maps of LFS 50 and HFS 50 conditions across all subjects. Columns indicate bins of trials (the first column is 1 to 10 trials, the second column is 11 to 20 trials, and the third column is 21 to 30 trials). The topography was the target band power.

**Table 2.** Correlation analysis between the classification accuracy (LFS 50 and HFS 50) and PSDs (alphaLow and alphaHigh).

Performance	AlphaLow(7.5 –9 Hz)		AlphaHigh (9 –12.5 Hz)	
	<i>r</i>	<i>p</i>	<i>r</i>	<i>p</i>
LFS 50	–0.6153	0.0008	–0.5172	0.0068
HFS 50	–0.0560	0.7858	–0.1178	0.5664

higher frequency (26–34.7 Hz). In this study, we confirmed the insignificant difference between visual fatigue and duty-cycle change by comparing duty-cycle differences of 50%, 60%, and 70% in higher frequency (26–34.7 Hz) stimuli conditions. However, different duty-cycle flickers resulted in slightly changed visual comfort and similar visual fatigue. The slight decrease in visual fatigue was statistically insignificant, in contrast to the findings of other studies, which reported that higher duty-cycles increased visual comfort.

The prediction of performance is an important topic in BCIs and spectral power in particular has been shown to be related to classification performance [47, 48]. Here, we predicted classification performance trends using neural signals such as alpha rhythms [45, 46] obtained from resting-state measurements. Across subjects, the performance of LFS 50 was highly correlated with the performance of HFS 50 ( $r = 0.7028$ ,  $p < 0.001$ ). However, the correlation with the alpha rhythm differed between LFS 50 and HFS 50 performance. We were only able to successfully predict the accuracy for low frequency stimuli using alpha power. Future work

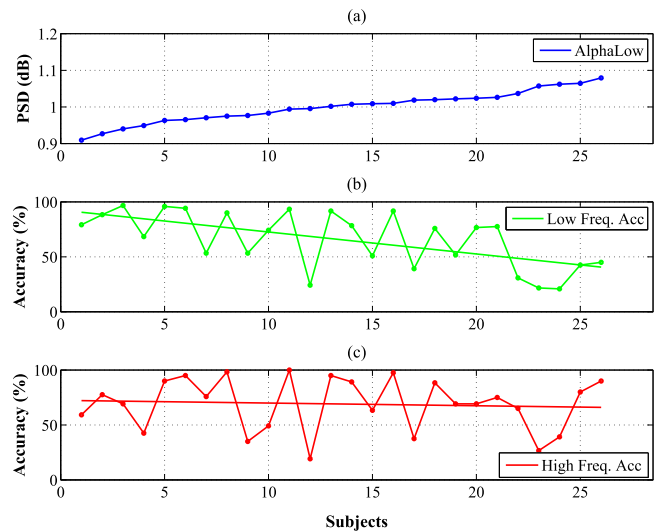


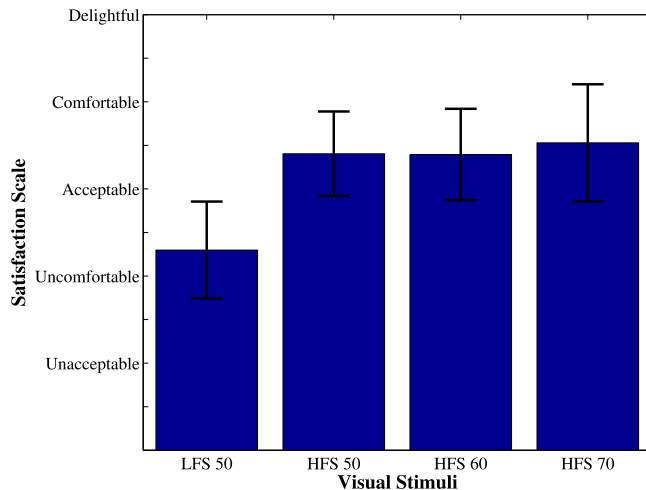
**Figure 9.** Comparison of classification performance and resting-state alpha activity. (a) The PSD of the alphaLow (7.5–9 Hz) band in ascending order by PSD. (b) LFS 50 accuracy trend in all subjects by alphaLow PSD. (c) HFS 50 accuracy trend in all subjects by alphaLow PSD.

will include an attempt to predict within-subject trial-to-trial BCI performance based on spectral features using non-linear regression techniques (e.g., [43, 44, 49–51]).

The self-reported questionnaire survey provided subjective feedback about visual fatigue [36, 52], which could be used to assess the relationship between visual fatigue and performance. Typically, participants demonstrate loss of

**Table 3.** Questionnaire survey of participants on visual feeling.

Stimulus	Unacceptable	Uncomfortable	Acceptable	Comfortable	Delightful
LFS 50	12	58	25	9	0
HFS 50	0	10	44	48	2
HFS 60	0	12	44	43	5
HFS 70	0	9	43	40	12

**Figure 10.** Comparison of visual fatigue scores obtained in the questionnaire survey. Higher scores indicate higher satisfaction.

attention to the experimental task when they are fatigued [53]. This is particularly important for increasing attention to enhance synchronization of SSVEP response [54]. Loss of attention and decreased arousal due to mental fatigue and/or distraction can significantly worsen SSVEP signal quality [55], as the SSVEP response is closely related to participants' visual fatigue and visual comfort [55]. Therefore, the difference in the SNR scale could indicate an objective measurement of visual fatigue, as SNR tends to decline as visual fatigue increases and a participant's concentration falls. Thus, the CCA values could be used as an objective measurement of visual fatigue in our study (figure 7(a)). In future studies, we will design objective measurements to further validate these visual fatigue results.

The mean classification performance obtained in this study ranged between 44% and 68.9% with the 15-channel set, which is lower than that reported in previous SSVEP-based BCI studies. However, a direct performance comparison is impossible due to different numbers of targets. In this study, we used 30 characters, resulting in a chance accuracy of 3.3%, but other studies used smaller numbers of targets (e.g., four [21] or 12 targets [56]). Another study, which first introduced a QWERTY-style SSVEP speller, showed an average classification accuracy of 87.58% over six subjects, which was attained after optimizing various factors, such as the distances between neighboring characters, light source arrangements, stimulation frequencies, electrode positions, and visual angles [13]. Because the main goal of this study was to investigate the effect of different stimulation

conditions on the usability of an SSVEP-based BCI system, we did not optimize any experimental factors that would lead to performance difference. We also recruited a larger number of subjects showing high intra-subject variability in performance, which could be another reason for the relatively low performance. Nevertheless, the trend of classification performance differences as time passes shown in this study was sufficient to investigate the variables of interest in our paradigm. In our future studies, we will design an online system to further validate our results in real-time BCI control situations.

## 5. Conclusions

In this study, we obtained improved visual comfort and achieved stable accuracy for an SSVEP-based BCI system using low frequency (6–14.9 Hz) stimuli and higher frequency (26–34.7 Hz) stimuli conditions. Our results revealed significant differences in different stimuli conditions in terms of performance trends and demonstrated significant improvements in the levels of visual comfort, as indicated by the questionnaire survey results. Our data suggest that using low frequency conditions as SSVEP stimuli results in unfavorable user fatigue that negatively affects user performance. The decrease in performance is significant, as performance could continue to worsen as time passes. Higher frequency stimuli conditions resulted in only slight changes to performance across time, and resulted in significantly better visual comfort. Thus, this study demonstrates that it is beneficial for users to adopt higher frequency stimuli in SSVEP-based BCIs, particularly in long-term use for practical applications.

## Acknowledgments

This research was supported by a National Research Foundation of Korea (NRF) grant funded by the Korea government (NRF-2015R1A2A1A05001867).

## References

- [1] Blankertz B, Dornhege G, Krauledat M, Müller K, Kunzmann V, Losch F and Curio G 2006 The Berlin brain-computer interface: EEG-based communication without subject training *IEEE Trans. Neural Syst. Rehabil. Eng.* **14** 147–52
- [2] Kim I-H, Kim J-W, Haufe S and Lee S-W 2015 Detection of braking intention in diverse situations during simulated

- driving based on EEG feature combination *J. Neural Eng.* **12** 016001
- [3] Kim J-H, BieBmann F and Lee S-W 2014 Decoding three-dimensional trajectory of executed and imagined arm movements from electroencephalogram signals *IEEE Trans. Neural Syst. Rehabil. Eng.* **23** 867–76
- [4] Yeom S-K, Fazli S, Müller K-R and Lee S-W 2014 An efficient ERP-based brain–computer interface using random set presentation and face familiarity *PLoS ONE* **9** e111157
- [5] Cecotti H 2011 Spelling with non-invasive brain–computer interfaces: current and future trends *Spelling with J. Physiology* **105** 106–14
- [6] Treder M S and Blankertz B 2010 (C)overt attention and visual speller design in an ERP-based brain–computer interface *Behav. Brain Funct.* **6** 1–3
- [7] Treder M S, Schmidt N M and Blankertz B 2011 Gaze-independent brain–computer interfaces based on covert attention and feature attention *J. Neural Eng.* **8** 066003
- [8] Yin E, Zhou Z, Jiang J, Chen F, Liu Y and Hu D 2013 A novel hybrid BCI speller based on the incorporation of SSVEP into the P300 paradigm *J. Neural Eng.* **10** 026012
- [9] Cecotti H 2010 A self-paced and calibration-less SSVEP-based brain–computer interface speller *IEEE Trans. Neural Syst. Rehabil. Eng.* **18** 127–33
- [10] Bin G, Gao X, Wang Y, Li Y, Hong B and Gao S 2011 A high-speed BCI based on code modulation VEP *J. Neural Eng.* **8** 025015
- [11] Volosyak I 2011 SSVEP-based Bremen-BCI interface—boosting information transfer rates *Journal of Neural Engineering* **8** 036020
- [12] Spüler M, Rosenstiel W and Bogdan M 2012 Online adaptation of a c-VEP brain–computer interface (BCI) based on error-related potentials and unsupervised learning *PLoS ONE* **7** e51077
- [13] Hwang H-J, Lim J-H, Jung Y-J, Choi H, Lee S W and Im C-H 2012 Development of an SSVEP-based BCI spelling system adopting a QWERTY-style LED keyboard *J. Neurosci. Methods* **208** 59–65
- [14] Yin E, Zhou Z, Jiang J, Yu Y-T and Hu D 2015 A dynamically optimized SSVEP brain–computer interface (BCI) speller *IEEE Trans. Biomed. Eng.* **62** 1447–56
- [15] Yin E, Zeyl T, Saab R, Chau T, Hu D and Zhou Z 2015 A hybrid brain–computer interface based on the fusion of P300 and SSVEP scores *IEEE Trans. Neural Syst. Rehabil.* **23** 693–701
- [16] Moore M M 2003 Real-world applications for brain–computer interface technology *IEEE Trans. Neural Syst. Rehabil.* **11** 162–5
- [17] Wang Y-T, Wang Y and Jung T-P 2011 A cell-phone-based brain–computer interface for communication in daily life *J. Neural Eng.* **8** 025018
- [18] Wang Y, Wang R, Gao X, Hong B and Gao S 2006 A practical VEP-based brain–computer interface *IEEE Trans. Neural Syst. Rehabil.* **14** 234–40
- [19] Bakardjian H, Tanaka T and Cichocki A 2010 Optimization of SSVEP brain responses with application to eight-command brain–computer interface *Neuroscience Lett.* **469** 34–8
- [20] Kwak N-S, Müller K-R and Lee S-W 2015 A lower limb exoskeleton control system based on steady state visual evoked potentials *J. Neural Eng.* **12** 056009
- [21] Diez P F, Mut V A, Perona E M A and Leber E L 2011 Asynchronous BCI control using high-frequency SSVEP *J. NeuroEng. Rehabil.* **8** 39
- [22] Regan D 1989 *Human Brain Electrophysiology: Evoked Potentials and Evoked Magnetic Fields in Science and Medicine* (Amsterdam: Elsevier)
- [23] Shyu K, Chiu Y, Lee P, Liang J and Peng S 2013 Adaptive SSVEP-based BCI system with frequency and pulse duty-cycle stimuli tuning design *IEEE Trans. Neural Syst. Rehabil.* **21** 697–703
- [24] Lee P-L, Yeh C-L, Cheng J-S, Yang C-Y and Lan G-Y 2011 An SSVEP-based BCI using high duty-cycle visual flicker *IEEE Trans. Biomed. Eng.* **58** 3350–9
- [25] Diez P F, Torres Müller S M, Mut V A, Laciár E, Avila E, Bastos-Filho T F and Sarcinelli-Filho M 2013 Commanding a robotic wheelchair with a high-frequency steady-state visual evoked potential based brain–computer interface *Med. Eng. Phys.* **35** 1155–64
- [26] Lin Z, Zhang C, Wu W and Gao X 2006 Frequency recognition based on canonical correlation analysis for SSVEP-based BCIs *IEEE Trans. Biomed. Eng.* **53** 2610–4
- [27] Molina G G and Mihajlovic V 2010 Spatial filters to detect steady-state visual evoked potentials elicited by high frequency stimulation: BCI application *Biomedizinische Technik* **55** 173–82
- [28] Yijun W, Ruiping W, Xiaorong G and Shangkai G 2005 Brain–computer interface based on the high-frequency steady-state visual evoked potential *Proc. of the 1st Int. Conf. on Neural Interface Control* (Piscataway, NJ: IEEE) pp 37–9
- [29] Mukesh T S, Jaganathan V and Reddy M R 2006 A novel multiple frequency stimulation method for steady state VEP based brain computer interfaces *Physiol. Meas.* **27** 61
- [30] Lalor E C, Kelly S P, Finucane C, Burke R, Smith R, Reilly R B and Mcdarby G 2005 Steady-state VEP-based brain–computer interface control in an immersive 3D gaming environment *EURASIP J. Appl. Signal Process.* **2005** 3156–64
- [31] Leow R, Ibrahim F and Moghavvemi M 2007 Development of a steady state visual evoked potential (SSVEP)-based brain–computer interface (BCI) system *Proc. of IEEE Int. Conf. on Intelligent and Advanced Systems* pp 321–4
- [32] Shan L R, Ibrahim F and Moghavvemi M 2007 Assessment of steady-state visual evoked potential for brain–computer communication *Proc. of the Int. Conf. on Biomedical Engineering* pp 352–4
- [33] Sami S and Nielsen K D 2004 Communication speed enhancement for visual based brain–computer interfaces *Proc. of the 9th Ann. Conf. of the International FES Society*
- [34] Tsoneva T, Garcia-Molina G, van de Sant J and Farquhar J 2013 Eliciting steady state visual evoked potentials near the visual perception threshold *Proc. of the 6th Int. IEEE/EMBS Conf. on Neural Engineering* pp 93–6
- [35] Regan D 1970 Evoked potential and psychophysical correlates of changes in stimulus colour and intensity *Vis. Res.* **10** 163–78
- [36] Volosyak I, Valbuena D, Luth T, Malechka T and Graser A 2011 BCI demographics II: how many (and what kinds of) people can use a high-frequency SSVEP BCI? *IEEE Trans. Neural Syst. Rehabil.* **19** 232–9
- [37] Zhu D, Bieger J, Molina G G and Aarts R M 2010 A survey of stimulation methods used in SSVEP-based BCIs *Comput. Intell. and Neurosci.* **2010** 1
- [38] Gao S, Wang Y, Gao X and Hong B 2014 Visual and auditory brain–computer interfaces *IEEE Trans. Biomed. Eng.* **61** 1436–47
- [39] Fisher R S, Harding G, Erba G, Barkley G L and Wilkins A 2005 Photic-and pattern-induced seizures: A review for the epilepsy foundation of america working group *Epilepsia* **46** 1426–41
- [40] Wickes J, Donchin E and Lindsley D 1964 Visual evoked potentials as a function of flash luminance and duration *Science* **146** 83–5
- [41] Bin G, Gao X, Yan Z, Hong B and Gao S 2009 An online multi-channel SSVEP-based brain–computer interface using a canonical correlation analysis method *J. Neural Eng.* **6** 046002

- [42] Bießmann F, Meinecke F C, Gretton A, Rauch A, Rainer G, Logothetis N K and Müller K-R 2010 Temporal kernel CCA and its application in multimodal neuronal data analysis *Mach. Learn.* **79** 5–27
- [43] Fazli S, Dähne S, Samek W, Bießmann F and Müller K-R 2015 Learning from more than one data source: data fusion techniques for sensorimotor rhythm-based brain-computer interfaces *Proc. IEEE* **103** 891–906
- [44] Dähne S, Bießmann F, Samek W, Haufe S, Goltz D, Gundlach C, Villringer A, Fazli S and Müller K-R 2015 Multivariate machine learning methods for fusing multimodal functional neuroimaging data *Proc. IEEE* **103** 1507–30
- [45] Zhang Y, Xu P, Guo D and Yao D 2013 Prediction of SSVEP-based BCI performance by the resting-state EEG network *J. Neural Eng.* **10** 066017
- [46] Acqualagna L, Bosse S, Porbadnigk A K, Curio G, Müller K-R, Wiegand T and Blankertz B 2015 EEG-based classification of video quality perception using steady state visual evoked potentials (SSVEPs) *J. Neural Eng.* **12** 026012
- [47] Blankertz B, Sannelli C, Halder S, Hammer E M, Kübler A, Müller K-R, Curio G and Dickhaus T 2010 Neurophysiological predictor of SMR-based BCI performance *NeuroImage* **51** 1303–9
- [48] Suk H-I, Fazli S, Mehnert J, Müller K-R and Lee S-W 2014 Predicting BCI subject performance using probabilistic spatio-temporal filters *PLoS ONE* **9** e87056
- [49] Dähne S, C F, Haufe S, Höhne J, Tangermann M, Müller K-R and Nikulin V V 2014 SPoC: a novel framework for relating the amplitude of neuronal oscillations to behaviorally relevant parameters *NeuroImage* **86** 111–22
- [50] Blankertz B, Lemm S, Treder M, Haufe S and Müller K-R 2011 Single-trial analysis and classification of ERP components—a tutorial *NeuroImage* **56** 814–25
- [51] Lemm S, Blankertz B, Dickhaus T and Müller K-R 2011 Introduction to machine learning for brain imaging *NeuroImage* **56** 387–99
- [52] Allison B, Luth T, Valbuena D, Teymourian A, Volosyak I and Graser A 2010 BCI demographics: How many (and what kinds of) people can use an SSVEP BCI? *IEEE Trans. Neural Syst. Rehabil.* **18** 107–16
- [53] Johns M W 2000 A sleep physiologist’s view of the drowsy driver *Transp. Res. F* **3** 241–9
- [54] Kim Y J, Grabowecky M, Paller K A, Muthu K and Suzuki S 2006 Attention induces synchronization-based response gain in steady-state visual evoked potentials *Nat. Neurosci.* **10** 117–25
- [55] Kaseda Y, Jiang C, Kurokawa K, Mimori Y and Nakamura S 1998 Objective evaluation of fatigue by event-related potentials *J. Neurological Sci.* **158** 96–100
- [56] Cheng M, Gao X, Gao S and Xu D 2002 Design and implementation of a brain-computer interface with high transfer rates *IEEE Trans. Biomed. Eng.* **49** 1181–6